Finite Element Analyses of Mortarless Wall Panel

N. A. Safiee, M. S. Jaafar, J. Noorzaie and M.R.A. Kadir

Department of Civil Engineering,
Faculty of Engineering
43400 UPM, Serdang
Selangor, Malaysia
Tel: 603-89464403
Email: norazizi@eng.upm.edu.my, msj@eng.upm.edu.my, jamal@eng.upm.edu.my

Abstract: The complexity of mortarless masonry wall behaviour was primarily governed by its dry joints characteristic. Dry joint features can be found in mortarless wall construction where no adhesive or mortar layer present. The behaviour of mortarless wall was addressed previously by experimental and analytical work. However there are lacks of research of analytical work particularly on the mortarless masonry wall considering dry joint features due to its complexity characteristic. Therefore this paper present finite element analyses on series of mortarless wall model. The analyses results then verified by comparing the results and response with those measured through experimental to monitor the accuracy and reliability of program. A 2D finite element program was developed to analyse dry joint masonry wall. The developed program was able to analyse linear and nonlinear problem. Four series of finite element wall model were developed that consists of solid hollow wall model, wall with stiffeners model, and wall with window opening models that simulate under various eccentricity of loading. The models were simulated in nonlinear environment and under compressive vertical load. The results show that the model was able to predict the correct response of mortarless masonry panels with good agreement and its demonstrated adequacy to provide reasonable results. [Report and Opinion. 2009;1(2):1-16]. (ISSN: 1553-9873).

Keywords: dry joint, masonry wall, finite element analysis, plane stress, compressive load

1.0 Introduction

Finite element method has been extensively used in analysing masonry structures and numerous models have been developed to simulate the behaviour of different types of the conventional mortared masonry systems [1 - 5]. Finite element technique is used to simulate the full masonry response under loading and also to implement the nonlinear solution procedure of the masonry system. However, analytical studies on the mortarless block systems are limited and depend mainly on the type of block used to assemble the walls. Interlocking mortarless load bearing hollow block wall is different from conventional mortared masonry systems in which the mortar layers are eliminated and instead the block units are interconnected through interlocking protrusions and grooves [5]. Putra block is one of interlocking block that can use in mortarless construction thus introducing dry joint interface between each block [13]. The dry joint characteristic of Putra block was assessing by experimentally which then extended to the analytical work [14]. Paulo [6] reported on experimental research on the structural behavior of dry joint masonry subjected to in-plane combined loading and also addressed a simplified method of analysis based on a continuum of diagonal struts. He also contributes the knowledge of dry joints under cyclic loading where focuses on the characterization of Coulomb failure criterion and the load-displacement behavior including aspects as surface roughness, dilatancy, and inelastic behavior [7]. However, there a lack of analytical work on the corresponding problem which related to dry joint of masonry. Therefore, this paper present analyses on the series of mortarless wall model using finite element analyses which then verified by comparing the results with those measured through experimental.

In this study, structural behaviors of mortarless wall system are accessed using 2D finite element program that specially developed to analyze this type of construction. A finite element model is proposed to predict the behaviour and failure mechanism of the wall system subjected to vertical compressive load. Mortarless wall system described here used Putra blocks develop by University Puta Malaysia as a main material. Then the analyses results are compared with existing experimental data in order to satisfy the validation process.

2.0 Proposed finite element model

The application of the finite element model has been shown by analysing mortarless wall constructed by interlocking hollow concrete block. Interlocking hollow concrete block used in this study known as Putra block invented by University Putra Malaysia. The following elements have been used to model masonry assemblage:

i. Eight-noded isoparametric plane element
ii. Six-nodded isoparametric interface element

The details of formulation of shape function of these elements can be obtained in [5]. Eight-noded isoparametric plane element is used to model masonry constituent (block). The eight nodes are located at the corners and mid side of each element as shown in Figure 1. Six-nodded isoparametric interface element of zero thickness located between material elements is employed to model the interface characteristics of the dry joint and bond between block and grout (if any). Three nodes are located on one side of the material element and the other three located on the other side as shown in Figure 1.

2.1 Proposed material model

In this study, the best fit equation of the experimental data of masonry block under uniaxial compression test for both ascending and descending parts is adopted [15]. It can be expressed as

$$\sigma = \frac{p\left(\varepsilon/\varepsilon_0\right)\sigma_0}{p-1+\left(\varepsilon/\varepsilon_0\right)^p} \qquad (1)$$

Where
σ, ε instantaneous values of the stress and the strain, respectively
σ_0, ε_0 the ultimate stress (peak) and the corresponding strain, respectively
p a constant called material parameter depends on the shape of the stress-strain diagrams

Other material properties that obtained from experimental work on dry joint behavior were normal stiffness, kn and shear stiffness, ks. Kn was given as follows

$$K_n = K_{ni} + Ad^B{}_n \qquad (2)$$

Where K_{ni} is the initial normal stiffness at zero stress and d_n is close up deformation. The close up deformation become main feature that makes the dry joint differs from the mortar joint under compressive load where the gradual closing-up of the space between the block to block surfaces.

2.2 Failure Criteria

The proposed model uses the biaxial compression strength envelope proposed by Vecchio [8]. The principal stresses on two orthogonal directions are denoted by σ_1 and σ_2 with $|\sigma_1| \leq |\sigma_2|$. The failures envelop is shown in Figure 2 for all stress states. For tension-compression region, the envelope relation that is used in this region can be written as

$$\sigma_{1p} = f_{eq} = \sqrt{1-\left(\sigma_2/f_c'\right)^2}\, f_t' \qquad (2)$$

$$\sigma_{2p} = \sigma_{1p}/\alpha \leq 0.65 f_t'$$

In which σ_{1p} tensile stress and σ_{2p} compressive stress
Where
f'_t is tensile strength of block unit
f_{eq} is equivalent tensile strength

3.0 Development of the finite element code

A Finite element program has been written in Fortran language and used as a main tool to analyse the mortarless wall model in this study. This program was developed to simulate the behavior of mortarless wall with special attention to simulating the contact behavior of dry joint interface.

Nonlinear analysis may be carried out using three methods; incremental or stepwise procedure, iterative and incremental-iterative technique (mixed technique). Mixed method or the incremental-iterative technique procedure has been adopted in the numerical solution due to the technique is possible to produce accurate results [5]. Fig. 3 shows solution procedure of the nonlinear analysis used in this study.

4.0 Finite element analyses mortarless masonry model

Four series of 2D finite element discretization model namely as Group A, B, C and D are developed in this study according to their specific accommodation of stiffeners arrangement in each wall as shown in. Group A models are considered for solid hollow wall without any stiffeners, Group B designated for wall model that having stiffeners over its perimeter and Group C is modelled for wall having stiffeners over its perimeter and at along length of mid height of wall. The developed models are based on the actual dimension of experimental panel constructed using Putra interlocking blocks. The size of panels used in this study are 3000mm x 1200mm x 150mm (height x length x thickness) for group A, B and C. For the group D, the size of panel used is 1500mm x 1600mm x 150mm with 600mm x 800mm of window opening located at the center of panel. The details of models to their corresponding group are shown in Table1. All models are simulated under the vertical compressive load that applied at top of wall. The loading is applied based on eccentricities considered as stated in Table 1. The wall models are idealized to span vertically by discretized the wall according its actual height and width. For the boundary condition the wall model is defined as fix and rolled at bottom and top of wall respectively. To define a fix condition in FE model, the translation of corresponding node need to restrain in x and y direction. For the application of roller condition, the translation in x direction needs to be restrained. Two dimensional (2D) finite element discretization of the wall in $x - y$ plane is adopted as shown in Fig. 4. Material properties used for masonry block and dry joint were based on actual experimental value are shown in table 2 and 3.

For the block, the typical properties are used to characterize the material properties such as E_o for initial elastic modulus, f'_c for compressive strength, f'_t for tensile strength and ν for poisson ratio. In this study, the best fit equation of the experimental data of masonry block under uniaxial compression test for both ascending and descending parts is adopted [5]. Trough this, the new features called material properties was introduced to consider the shape of the stress strain diagrams known as p in equation 1.

5.0 Results and Discussion

The results are presented in term of their maximum load, vertical displacement and lateral displacement along height corresponding to respective eccentricities.

5.1 Wall compressive strength

Table 2 shows the predicted strength of the walls associated with the corresponding available experimental test results. The used eccentricity range (from e = 0.0 to e = 55mm) can be divided into three regions, axial and lower eccentricity region, middle eccentricity region and higher eccentricity region. The comparison between the predicted and test results of wall compressive strength of three groups shows that the predicted capacities are quite close to the test results. The discrepancies between the FE model and the test results are varied from -0.68% to 22% which also shown in Table 2. The predicted maximum load that obtained by FE models are over estimated for lower and medium eccentricities. However, the FE model showed a reduction in the wall capacity in the higher eccentricity especially in the Groups A and C. This is due to tensile stress produced in tension side of the wall which caused opening in the mortarless joints and reduced the wall capacity. This is also may due to the flexural effect that governed by FE model in the higher eccentricity. However, FE model of D1 predicted well the compressive strength of wall where it gives same results as those measured by experimental.

5.2 Axial deflection

Figure 5 to 8 shows the results of vertical deflection of walls Group A to Group D for both experimental and finite element analyses. The results are presented for zero eccentricity. All the walls are loaded axially

until failure and the results of vertical displacement over load are plotted. Results of un-stiffened wall of Group A as shown in Fig 5 shows that nonlinear relationship are govern by both measurement of experimental [9] and FE. From the figure, it shows a good prediction in term their response for both measurements. The FE deflection shows limited deflection compared to those measured by experimental. This is may be due to uneven surface of block where caused the deformation of un-stiffened wall leading to the nonlinear progressive contact deformation of the dry joint interface which reveals extensive deformation at the lower load level. Deflection of both measurements was in good agreement in the first loading but became scatter when loading increased. The differences of results were in the range 14 to 39%. Deflection measured by experimental shows the value increased with higher magnitude for each loading increment. However FE seems to have a limited deflection even though could achieve higher load. Maximum deflection that could achieve by FE was 5mm. This is may be due to the application of boundary condition at top of FE model where may not allow more deflection.

Fig. 6 shows the vertical displacement results of wall with stiffeners over its perimeter represent by Group B. The finite element results were compared with the experimental results that tested by Fares [10]. The response that predicted by FE was different compared with experimental results. The initial extensive deformation was shown by FE results, but it does disappear in the experimental results. This behaviour due to the simplicity taken by FE model which consider the existing of grout only and not include the steel reinforcement in modeling. However the existing of stiffeners also affected the overall behavior of the walls by produced better deformation compared than unstiffeners wall. The deformation was controlled by the weight of wall where in stiffeners wall it tend to response as assemblage of unit to large entity thus results more deformation and also eliminate the effect of dry joint. FE model was overestimated the deflection in initial of loading, but it seems to approach the experimental values when the load reach 300 kN. It can be seen that, using vertical stiffeners reduces the maximum vertical deformation to 3.78 mm as predicted by FE model. This value was 23% of maximum vertical deformation of the un-stiffened walls. The reduction of the vertical deformation in stiffened walls compared to the unstiffener wall was also confirmed by the test results.

Fig.7 shows the vertical deflection of stiffened wall C1 of Group C. The response of deflection of C1 was similar to B1 where FE model overestimate the prediction of deflection at early stage of loading. However the predicted deflection by FE was decreasing by load until it meets the experimental deflection value at 400kN. This is may be due to existing of stiffeners at middle height of wall and crushing of the grout of stiffeners where causing deflection rate reduced. The response that predicted by FE explained that the model having a ductility. It can be seen that, by using vertical stiffeners the deformation is reduces the maximum vertical deformation to 4.7mm in wall C1 as predicted by the FE model. This value is 22% of the maximum vertical deformation of the un-stiffened walls. As shown in Fig. 7, comparable results have been obtained by the FE model and the experimental test results of wall C1. The initial stiffness of the wall was relatively overestimate predicted by the numerical model curves however it closely predicted the stiffness at higher loads. The reduction of the vertical deformation in stiffened walls compared to the un-stiffened wall was also confirmed by the test results. It can be shown that the effect of the horizontal middle stiffeners is limited on the vertical deformation of wall C1 compared to B1.

Fig. 8 shows the results of vertical deformation of wall with opening for both finite element and experimental measurement [12]. The results are shows good agreement at initial stage of loading and results in good response. However, remarkable differences in deformation could be observed in higher loading before bridging back nearly at failure load. The deformations that predicted by finite element seems to has a limited capacity compared to the experimental values. This is may be due to developed model has higher stiffness. Other than that, the roughness of block in experimental specimens also may influence the deformation of wall. The behavior that obtained by experimental mainly due to the variation in the contact behavior of dry joints that was affected by the geometric imperfection caused by block bed irregularity and variation of block height [5]. This will affect the full seating by each block in wall. The stiffness that obtained by finite element also more higher compared to the experimental thus giving that the developed model able to predict the response of wall with opening but with the limited capacity of deformation.

5.3 Lateral deflection

The variation of predicted lateral deflection along the wall height near the failure load for un-stiffened walls A2 and A3 are respectively shown in Fig. 9 and 10. As it is clearly shown in the figures, the wall panel that loaded in more eccentricity (e = 55 mm) revealed higher lateral deformation than in the less

eccentricity (e = 40mm) loaded walls due to the flexural effect of eccentric loads. The similarity between the FE model analysis and test results is distinct which indicates accurate simulation for lateral deformation of wall by the developed FE model. This is reflecting the block beds geometric imperfection that incorporates into the FE model. The discrepancies between the FE predicted maximum deflection are varied from -38% to 19% of the experimental maximum deflection.

Fig. 11 to 12 shows the variation of lateral deflection along the walls height near the failure load for the stiffened walls B2 and B3 respectively. With exception of wall B1 the lateral deflection along the walls height are closely predicted by the model. The differences between the predicted and the corresponding test result are varied between -15% and -53%. This behavior is due to the initial imperfection along the wall height observed in the experimental setup which affected the deflected shape and also the wall capacity. Perceptible reduction occurred in the magnitude of lateral deformation of the eccentrically loaded walls in the stiffened walls compared to the unstiffened wall due to the vertical stiffeners. The predicted reduction by the numerical model in the walls loaded with eccentricity of 55mm reaches 57%. In the stiffened walls, deflected shape and location of the maximum deflection are affected highly by the unsymmetrical boundary condition at the top and bottom of the analyzed walls.

Fig. 13 shows the variation of lateral deflection over wall height of stiffened walls C3. The lateral deflections along the walls height are closely predicted by the model as shown in Fig. 12. The variation of results may be due to the initial imperfection along the wall height observed in the experimental setup which affected the deflected shape and also the wall capacity. The differences of lateral deflection are higher in mid height region due to flexibility of interlocking unit and may also influence by flexural effect of wall. The differences between the predicted and the corresponding test result are varied between -3% to 45%. Perceptible reduction occurred in the lateral deformation of the eccentrically loaded walls in the stiffened walls compared to the un-stiffened wall due to existing the vertical and horizontal stiffeners. The predicted reduction by the numerical model in the walls loaded with eccentricity of 55mm reaches 58% in Group C compared to Group A.

Table1 Designation of wall model according to their group

Group	Designation	Eccentricity (e) mm
A	A1	0
	A2	40
	A3	55
B	B1	0
	B2	40
	B3	55
C	C1	0
	C2	55
D	D1	0

Table 2 Dry joint material properties

Joint	K_{ni}, N/mm^3	K_s, N/mm^3	Coefficient A	Coefficient B
Dry joint	5.0	1000	282.2	2.01

Table 3 Masonry block material properties

Type of material	E_o,, N/mm^2	f'_c, N/mm^2	ε_o	Material parameter	f'_t, N/mm^2	Poisson ratio, ν
Concrete block	9050.7	-18	-0.0021	2.5	1.98	0.2

Table 4 Predicted strength of wall by FE

Group	Designation	Eccentricity (e) mm	Max comp. load (kN) FE	Max comp. load (kN) Experimental	Discrepancy %
A	A1	0	476	373	5
	A2	40	338	322	-4
	A3	55	271	283	
B	B1	0	600	532	11
	B2	40	570	460	19
	B3	55	400	395	1
C	C1	0	600	615	-3
	C2	55	440	443	-0.68
D	D1	0	450	450	

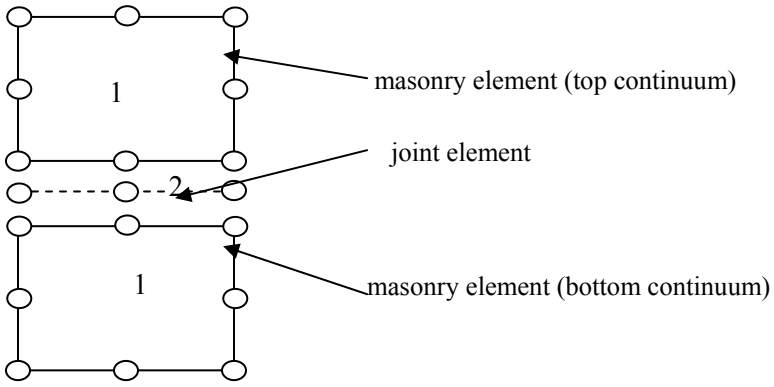

Figure 1. Masonry and interface joint element

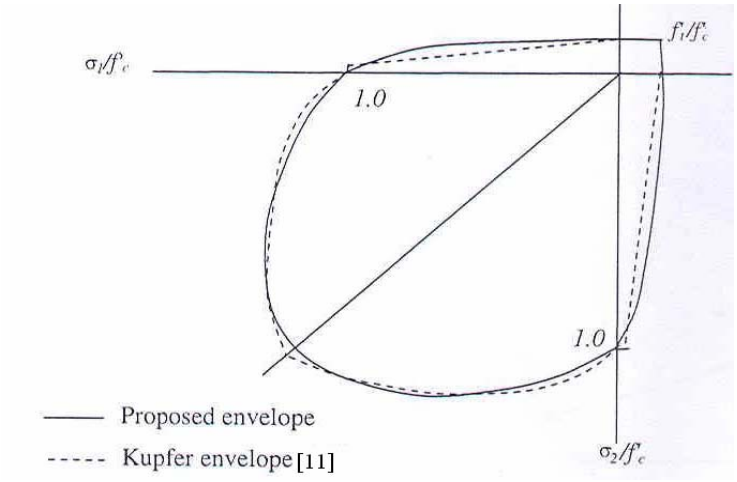

Figure 2 Masonry Failure envelope for different stress state

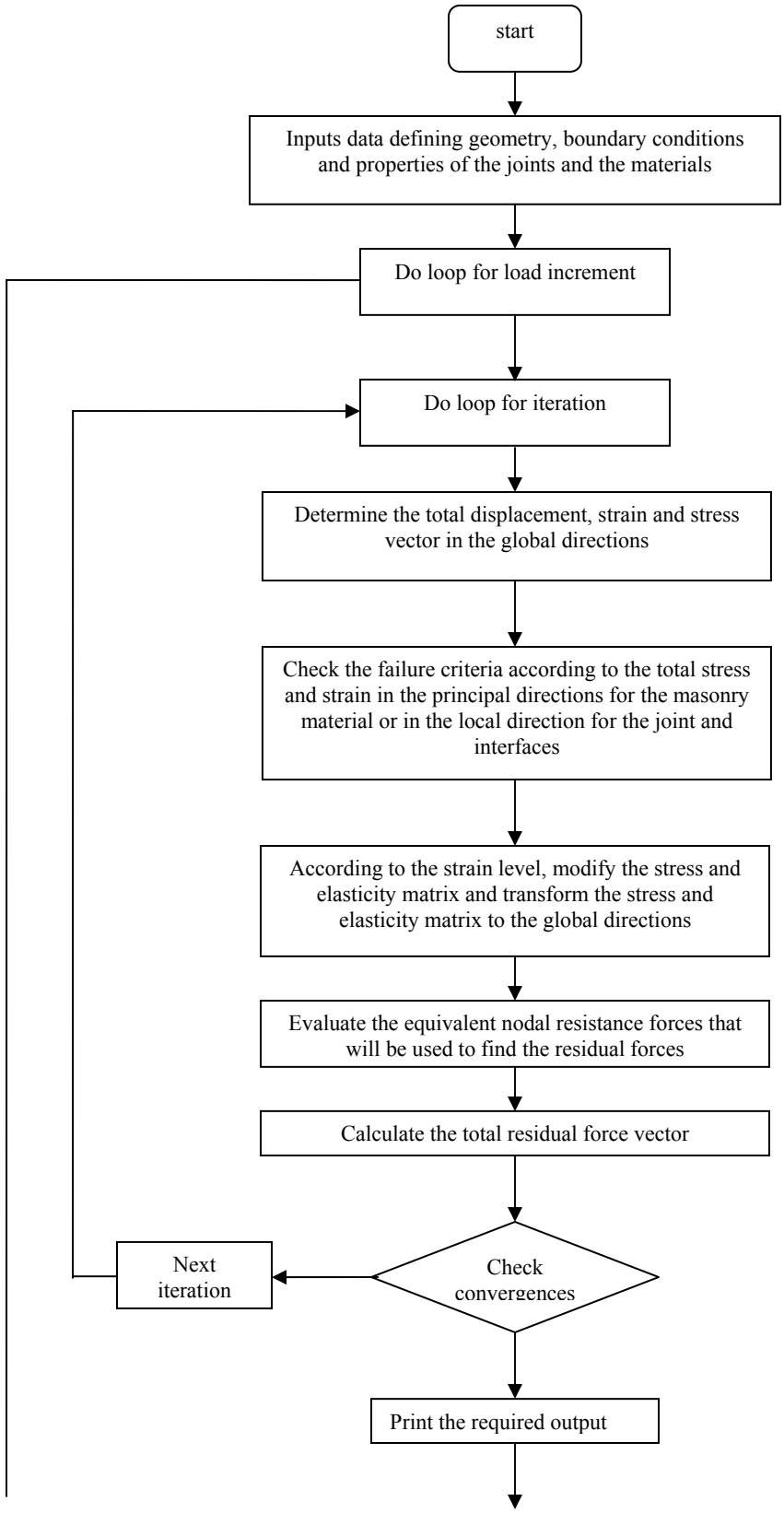
start
Inputs data defining geometry, boundary conditions and properties of the joints and the materials
Do loop for load increment
Do loop for iteration
Determine the total displacement, strain and stress vector in the global directions
Check the failure criteria according to the total stress and strain in the principal directions for the masonry material or in the local direction for the joint and interfaces
According to the strain level, modify the stress and elasticity matrix and transform the stress and elasticity matrix to the global directions
Evaluate the equivalent nodal resistance forces that will be used to find the residual forces
Calculate the total residual force vector
Check convergences
Next iteration
Print the required output

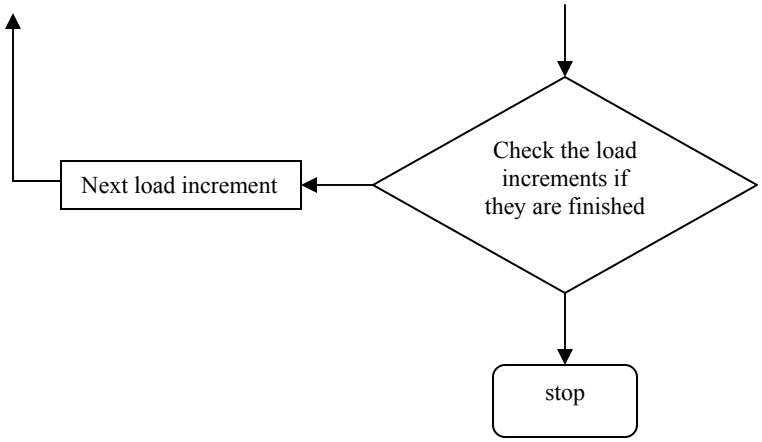

Figure 3 Solution procedure of the nonlinear analysis [5]

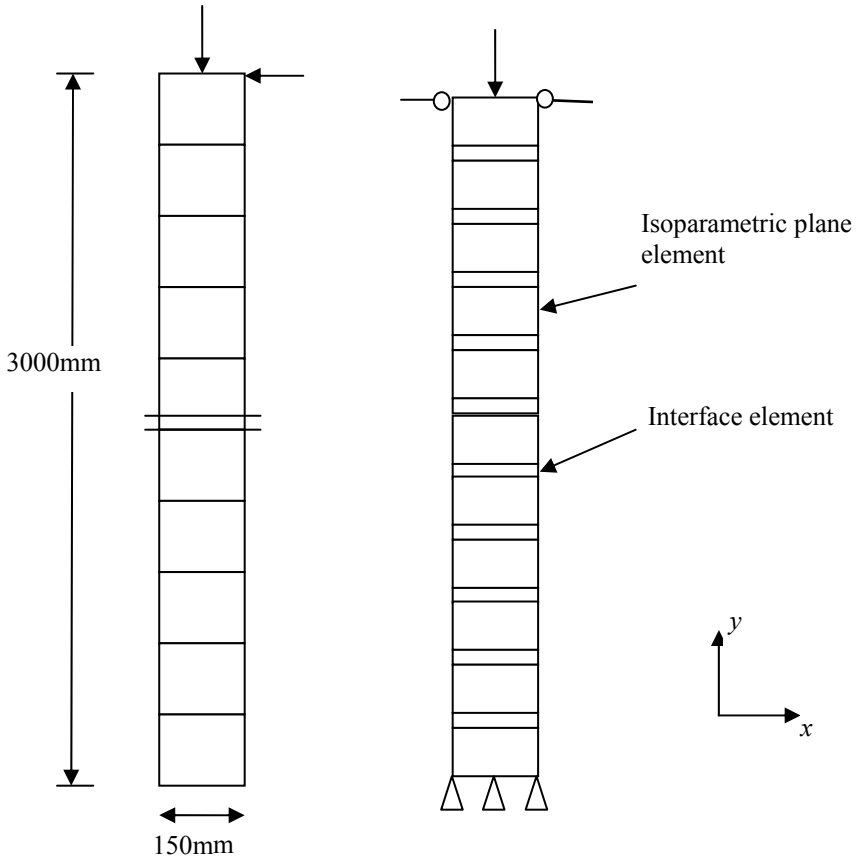

Figure 4 2D finite element discretization of wall model

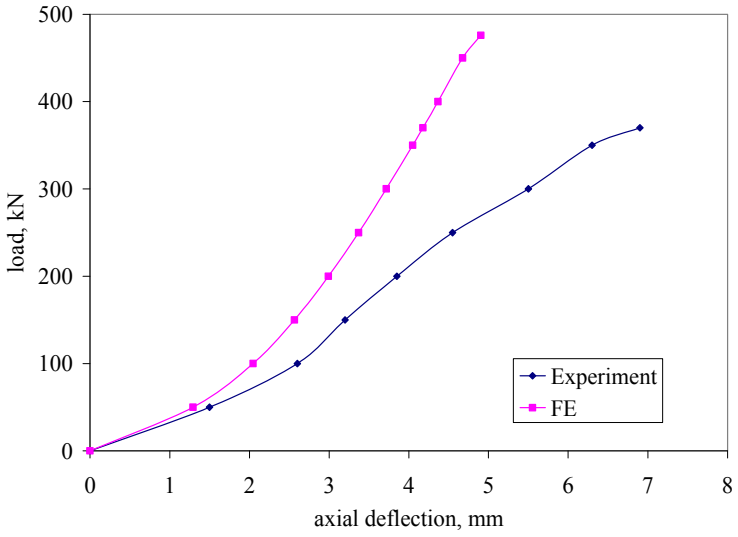

Figure 5 Load vs axial deflection of A1

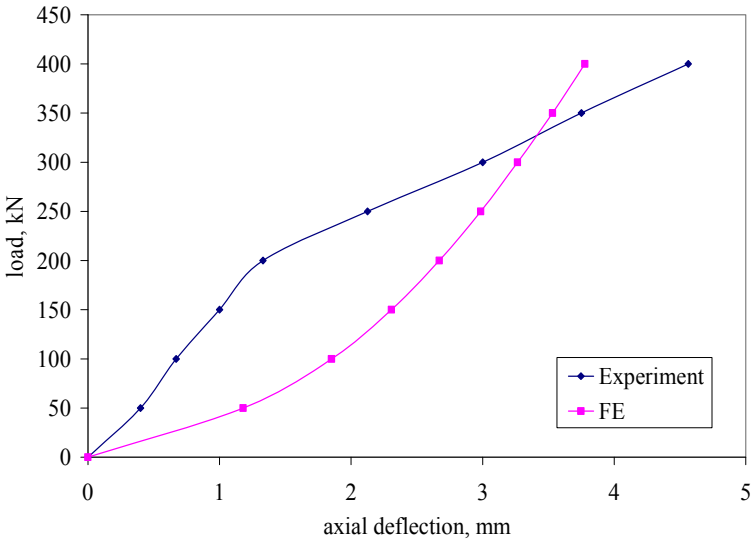

Figure 6 Load vs vertical deflection of B1 wall

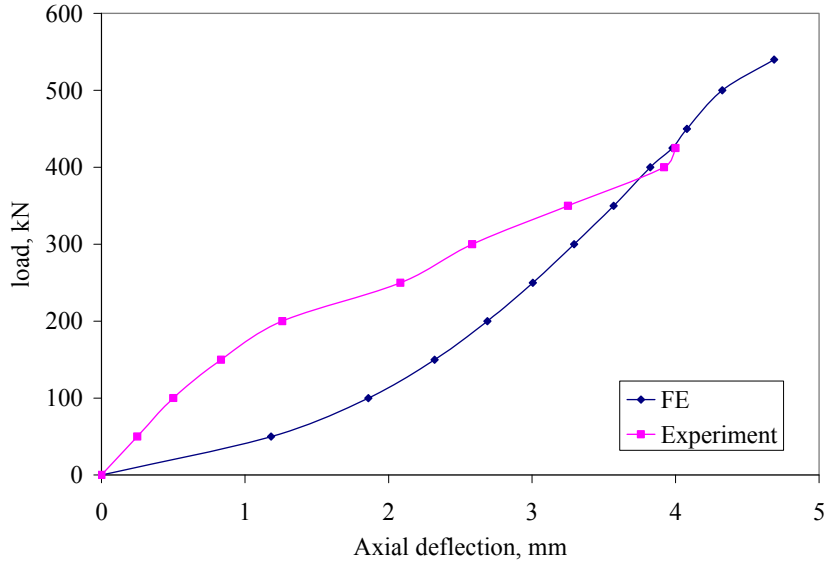

Figure 7 Load vs vertical deflection of C1

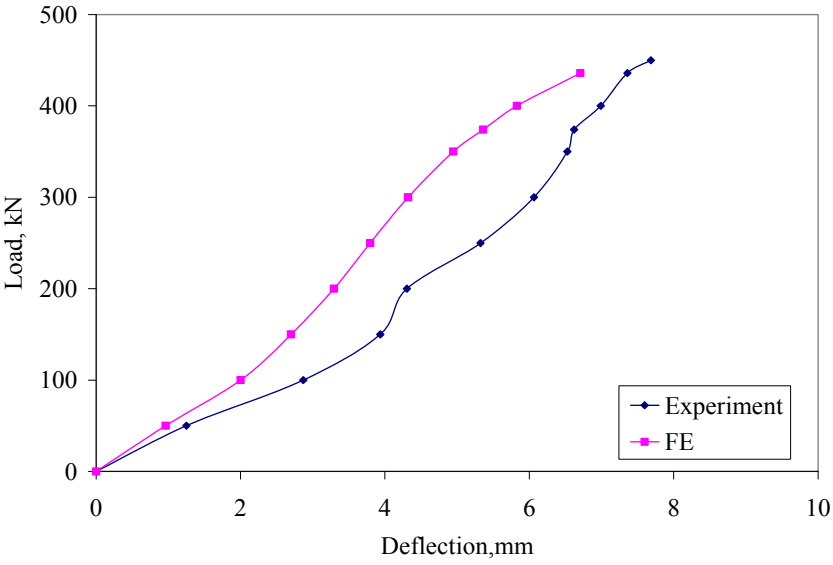

Figure 8 Vertical deformation of wall D1

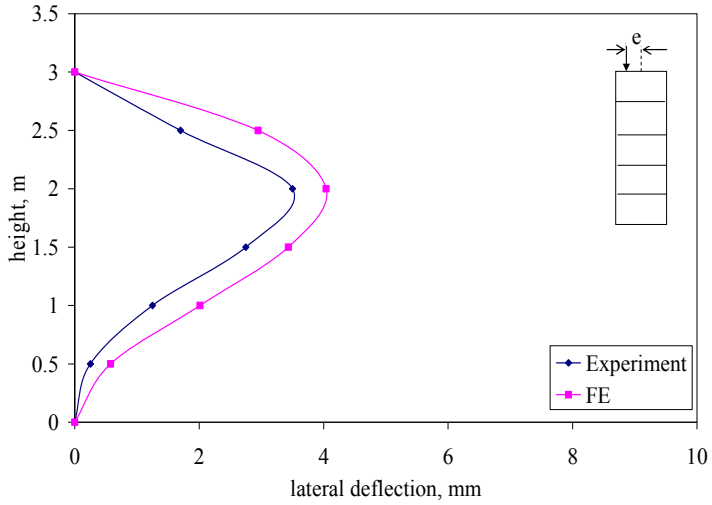

Figure 9 Lateral deflection over height of A2 (e = 40 mm)

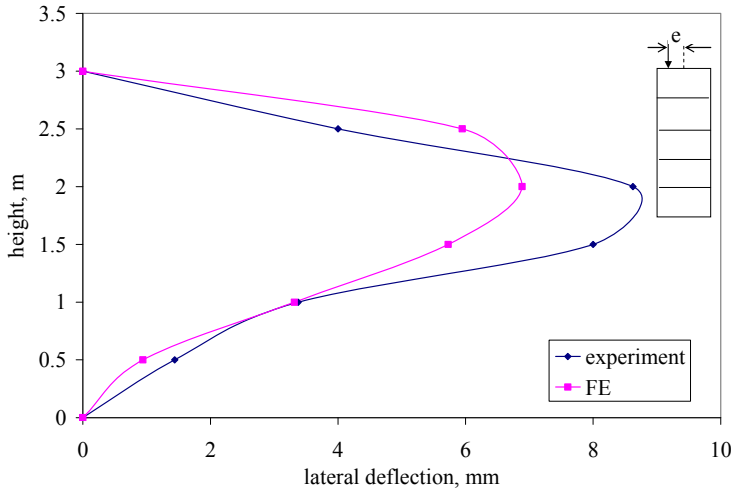

Figure 10 Lateral deflection over height of A3 (e = 55mm)

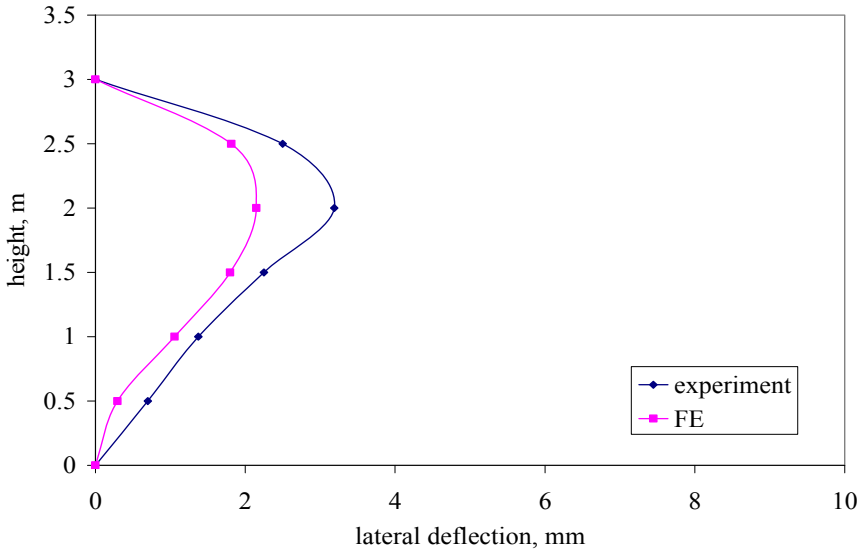

Figure 11 Lateral deflection over height of B2 (e = 40 mm)

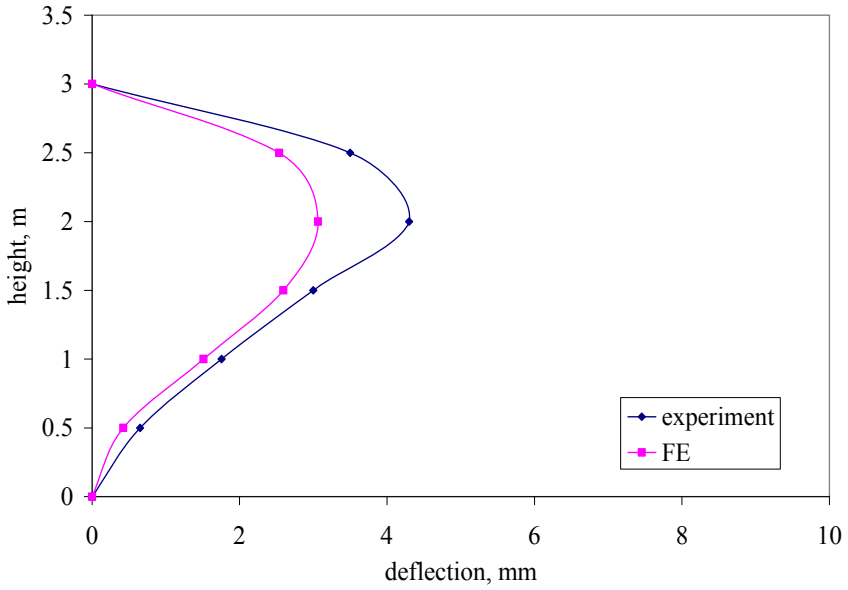

Figure 12 lateral deflection over height of B3 (e = 55mm)

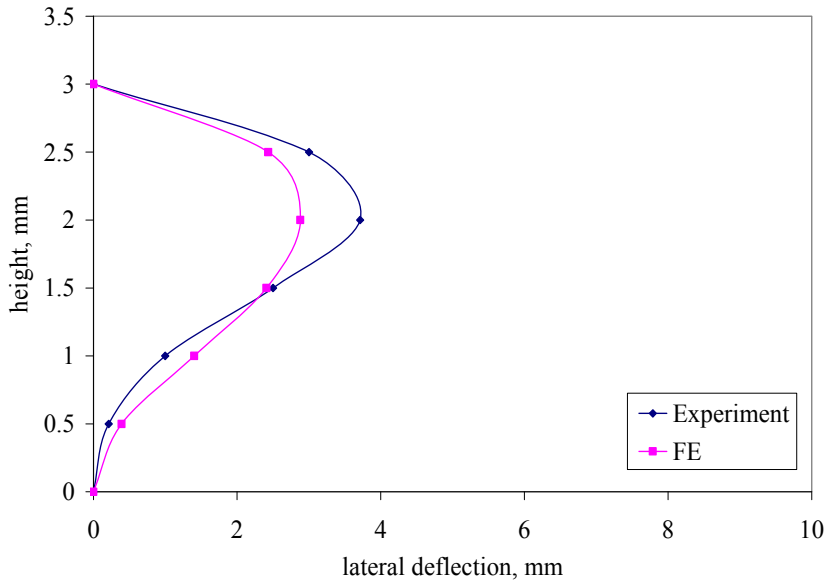

Figure 13 Lateral deflection of C3 (e = 55 mm)

6.0 Conclusion

The paper presents experimental results on the validation study between developed finite element model and available experimental data. Based on the results obtained, the models are able to predict the correct response of mortarless masonry panels subjected the vertical compressive load. A finite element analysis of model demonstrated its adequacy to provide reasonable results. For the group A, the variation of predicted lateral deflection along the height for the un-stiffened exhibit good agreement in term their response for both measurements with slightly differences in the range 14% to 39%. While for stiffened walls the lateral deflection of wall were closely predicted by the model. Perceptible reduction occurred in the lateral deformation of the eccentrically loaded walls in the stiffened walls compared to the unstiffened wall due to the vertical stiffeners. The wall panel that loaded eccentrically revealed higher lateral deformations than the axially loaded walls due to the flexural effect of eccentric loads. The similarity between the finite element model analysis and test results is distinct which indicates accurate simulation for lateral deformation of wall by the developed finite element model. Therefore, the finite element program can be used for further work as a tool to predict or to obtain the database for development of design method for mortarless wall masonry.

References

[1] Alpa, G., Monetto, I. 1994. Microstructural Model for Dry block Masonry Walls with In-plane Loading. Journal of the Mechanics and Physics of Solids. 42 (7): 1159-1175

[2] Andreaus, U. 1996. Failure Criteria for Masonry panels under In-Plane Loading. Journal of Structural Engineering. 122 : 37- 46

[3] Wang, R., Elwi, A.E., Hatzinikolas, M.A. 1997. Numerical study of tall masonry cavity walls subjected to eccentric loads. Journal of Structural Engineering. 123: 1287 – 1294

[4] Kwan, A.K.H., He, X.G. 2001. Finite Element Analysis of Effect of Concrete Confinement on Behavior of Shear Walls. Computers and Structures. 79: 1799-1810

[5] Alwathaf, A.H. 2006. Development of finite element code for non-linear analysis of interlocking mortarless masonry system, PhD thesis, Civil Engineering Department, University Putra Malaysia

[6] Lourenco, P.B., Oliveira, D.V., Pere Roca, P., and Orduna, A. 2005. Dry Joint Stone Masonry Walls subjected to In-plane combined loading. Journal of Structural Engineering. 131: 1665-1673

[7] Lourenco, P.B., and Ramos, L.F. 2004. Characterization of Cyclic Behavior of Dry Masonry Joints. Journal of Structural Engineering. ASCE. 130: 779 - 786

[8] Vecchio F. 1992. Finite element modelling of concrete expansion and confinement. Journal Structural Engineering. ASCE. 118 : 2390-405

[9] Amad M.S. Najm. 2001. Structural behaviour of load-bearing interlocking hollow block masonry, Master thesis, Universiti Putra Malaysia

[10] Fares A. Shehab. 2005. Structural behaviour of Interlocking hollow block panel with stiffener subjected to axial and eccentric load, Master thesis, Universiti Putra Malaysia

[11] Kupfer H., and Gerstle K, 1973. Behaviour of concrete under biaxial stresses. Journal of Engineering Mechanics Division. ASCE. 99: 853-867

[12] Labeb. 2008. Behavior of Interlocking Hollow block Wall with Opening, Master Thesis, University Putra Malaysia

[13] Thanoon, W.A., Jaafar M.S., Abdul K.M.R., Ali, A.A., Trikha, D.N. and Najm, A.M. 2004. Development of an innovative interlocking load bearing hollow block system in Malaysia. Construction and Building Materials. 18:445-454

[14] Thanoon, W.A., Alwathaf, A.H., Noorzaei, J., Jaafar, M.S., Kadir, M.R.A. 2008. Nonlinear finite element analysis of grouted and ungrouted hollow interlocking mortarless block masonry system. Engineering Structures. 30: 1560-1572

[15] Carreira, D.J and Chu, K.C.1985. Stress-strain relationship for plain concrete in compression. ACI Journal. 32: 797-804

12/22/2008